International Journal of Scientific Research & Engineering Technology (IJSET)
Vol.14 pp.16-21

Modeling of thermal fluid transport phenomena in laser welding of a hetergenous assembly

Sabrine BEN HALIM[1], Sana BANNOUR[1], Kamel ABDERRAZEK[1], Wassim KRIAA[1], Michel AUTRIC[2]

[1]*University of Monastir, National Engineering School of Monastir, Laboratory of Thermal and Thermodynamics of Industrial Processes*
5000.Monastir. Tunisia
[1]sabrinebenhalim8@gmail.com
[2]*Aix-Marseille Univ, CNRS, IUSTI*
Marseille, France
[2]michel.autric@univ-amu.fr

Abstract— **The laser welding is a technique of joining different materials which consists in melting the metal under the effect of laser radiation and creating a weld joint. It is an important process to assembly dissimilar materials. In this work, a three-dimensional multiphysical transient model was developed from the solution of the equations of mass, momentum, energy conservation and solute transport in the weld pool. This numerical model made it possible to simulate the heat transfer, fluid flow and distribution of elements in dissimilar laser welding of Al / Mg. The isothermal surfaces are simulated to study the transient temperature distribution and thermal cycles at different regions. The distribution of chemical elements of Al and Mg and the composition profile are also studied. It is shown that heat transfer and mass transport are two main phenomena in the formation of a heterogeneous mixture in the melting zone. The results given by the numerical simulation are in good agreement with the corresponding experiments, using the same process input parameters.**

***Keywords*— numerical investigation, dissimilar metals, thermal cycle, fluid flow, mass transport**

I. INTRODUCTION

Nowadays, several manufacturers in the automotive and aeronautics fields have studied the use of light metal alloys in different welding processes. This would allow them to reduce the weight of their mobile gear, or the reduction of energy consumed, and therefore the emission of gaseous pollutants. Recently, the use of Magnesium and Aluminum alloys has invaded the transportation industries thanks to their interesting characteristics. Aluminum alloys are characterized by low density, good corrosion resistance, high thermal and electrical conductivity [1, 2], potential recovery, durability, inexpensive maintenance [3] and recyclability [4]. For Magnesium alloys, they have high strength [5], good moldability, hot forming and recycling [6]. However, it has been found that joining of dissimilar metals Al and Mg presents difficulties because of the difference in thermal and physical properties, the formation of brittle intermetallic compounds extremely fragile in the transition zone between the two materials and the presence of cracks in the joint [5,7].

Several similar and dissimilar material welding techniques such as electron beam welding [8], MIG welding [9, 10], resistance spot welding [11], bonding diffusion [12, 13] have been studied. Other studies have focused on laser welding. For example, Chen et al. [14] studied experimentally and numerically the laser welding of Titanium / Aluminum joints. They have highlighted more particularly the inhomogeneous mixture which can be formed during the welding process. G. Casalino et al. [15] studied numerically the fiber laser welding of Ti6Al4V and AA5754-T40 materials using the Ansys Parametric Design Language (APDL). They studied the effect of some welding conditions on thermal behavior. K. S. Kumar et al. [16] developed a three-dimensional numerical model based on the finite element method using COMSOL multiphysics software to study the butt welding of AISI 316L stainless steel sheets by a pulsed laser beam. They used a heat source with a Hermit Gaussian rectangular spatial distribution. The distribution of the temperature at the level of the welded joint shows the creation of the plasma around the heat source, then, a rapid decrease in the temperature in the direction of the radiation of the laser source. M. F. X. Muthu [17] carried

ISSN 1737-9296

out an experimental study of Aluminum/Copper alloys by friction stir welding. They used three different pin profiles. They analyzed the microstructure and the mechanical properties. They have found that the use of plain taper pin profile in the welding process gives better elasticity and tensile strength. G. Qianqian et al. [18] carried out the welding of low carbon steel to 6016 Aluminum alloy by fiber laser. They found that the welding speed plays an important role in the formation of the molten pool. In fact, the increase in speed leads to an increase in the depth of penetration. As a result, solute islands are formed and promote the appearance of cracks in the weld joint.

This paper deals with numerical analysis of temperature, velocity fields and mass fraction distribution by laser welding process of Magnesium alloy to Aluminum alloy using finite volume code. The 3D model predicts also the weld bead geometry. The simulated results are validated the same with the corresponding experimental results.

II. Experimental procedure

In this numerical modeling, the Aluminum alloy and the Magnesium alloy were used as base metals. The chemical compositions of these alloys are shown in table I. In this experiment, Aluminum alloy was arranged above Magnesium alloy, Figure 1. The experiments were performed with a continuous Yb: YAG laser with a wavelength of 1032 nm. The radius of the laser beam is 0.45 mm [19]. An Argon shielding gas with a flow rate of 20 l / min was used to protect the weld bead from oxidation. The thermo-Physical properties of the base materials are shown in table II and the operating parameters used in this work are shown in Table III.

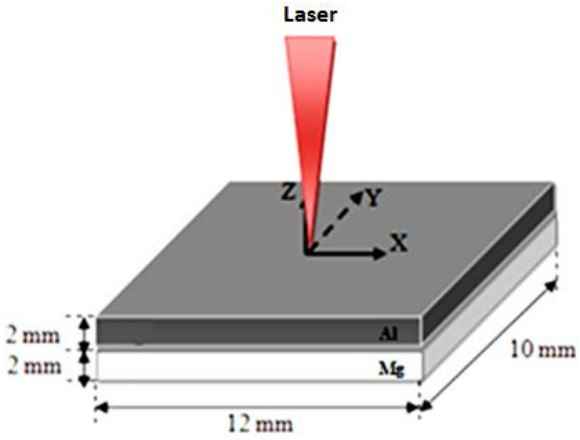

Fig. 1 Adopted lap joint configuration

TABLE I. Chemical composition of base materials

Chemical Elements	Mg	Al	Mn	Zn	Fe	Cu	Si
Magnesium	96.67	2.65	0.17	0.52	…	…	…
Aluminum	2.68	96.63	…	…	0.4	0.14	0.13

TABLE II. Characteristics of base metals

Property	Magnesium	Aluminum
Density (solid state) [kg/m^3]	1810	2880
Thermal conductivity (solid state) [W/m·K]	146	202
Specific heat (solid state) [J/Kg·K]	1020	728
Solidus temperature [k]	880	740
Liquidus temperature [k]	933	923

TABLE III. Welding parameters adopted in numerical analysis

Configuration	Laser power (w)	Welding velocity (m/s)
Al/Mg	2500	0.66

III. Numerical simulation

Heat transfer, fluid movement, and mass transport during laser lap welding of dissimilar Aluminum / Magnesium materials were simulated by 3D transient numerical model. The dimensions of the computed domain are 12 mm × 10 mm × 4 mm. The calculation was carried out with a mesh composed of 1170,000 cells. We have adopted a uniform mesh over the entire area of

ISSN 1737-9296

computation and refined mesh near the heat source. The workpiece moves with a constant speed U_x.

The assumptions adopted are as follows:

- The model is unsteady.
- The physical properties vary with temperature and mass fraction.
- Liquid flow in the molten pool is laminar and incompressible.
- The free surface of the weld pool is flat.

IV. EQUATIONS

This study is based on the resolution of conservation equations expressed as follows [9]:

Mass conservation

$$\frac{\partial(\rho)}{\partial t} + \nabla.(\rho\vec{v}) = 0 \quad (1)$$

Where $\vec{v}$ is the speed following the respective directions.

Momentum conservation

$$\frac{\partial(\rho\vec{v})}{\partial t} + \nabla.(\rho\vec{v}\vec{v}) = -\nabla p + \nabla.(\mu\nabla\vec{v}) + \rho\vec{g} + \vec{S} \quad (2)$$

Where p is the pressure, μ is the viscosity and $\vec{S}$ is the source term.

Energy conservation

$$\frac{\partial(\rho H)}{\partial t} + \nabla.(\rho\vec{v}H) = \nabla.(k\nabla T) + S_E \quad (3)$$

Where H is the enthalpy and S_E is the energy source term.

Species conservation

$$\frac{\partial(\rho C)}{\partial t} + \nabla.(\rho\vec{v}C) = \nabla.(\rho D\nabla C) \quad (4)$$

Where C is the concentration and D is the mass diffusivity.

The heat flow and fluid flow models were coupled with a melting and solidification model. Melting and solidification of the weld pool was simulated with an enthalpy-porosity formulation. It indicates the liquid fraction in the weld pool. The mushy region, partially solidified region was treated as a porous medium.

The momentum sink due to the reduced porosity in the mushy zone can be expressed as:

$$\vec{S} = -\left(\frac{A(1-\beta)^2}{\beta^3+b}\right)\vec{v} \quad (5)$$

Where ε is the liquid fraction, A is the mushy zone constant (a large number, say 10^8) and b is an arbitrary small number to prevent division by zero (10^{-3}).

V. BOUNDARY AND INITIAL CONDITIONS

At time t = 0s, the entire domain was considered to be in the solid state with a temperature of 300 K and the gravitational acceleration was assumed to be 9.81 ms^{-2}.

At the free surface of the liquid, shear force due to surface tension is expressed as:

$$\mu\frac{du}{dz} = \beta\frac{\partial\sigma}{\partial T}\frac{\partial T}{\partial x} + \beta\frac{\partial\sigma}{\partial C}\frac{\partial C}{\partial x} \quad (6)$$

$$\mu\frac{dv}{dz} = \beta\frac{\partial\sigma}{\partial T}\frac{\partial T}{\partial y} + \beta\frac{\partial\sigma}{\partial C}\frac{\partial C}{\partial y} \quad (7)$$

Where σ_T is the thermal surface tension coefficient.

The heat loss by convection heat transfer and radiation is given by,

$$q_{rad} = \varepsilon\sigma(T^4 - T_0^4) \quad (8)$$

$$q_{conv} = h_{conv}(T - T_0) \quad (9)$$

Where h_{conv} is the convection coefficient, σ is the Stefan-Boltzmann constant and ε is the emissivity of the surface radiation.

VI. RESULTS AND DISCUSSION

The predicted temperature and velocity distributions, composition profile are investigated and compared with experimental results in the following sections

Figure 1 illustrates the distribution of isotherms of different surfaces of welding joint. These isotherms are linked to thermal melting-solidification cycles characteristic of the laser welding process. Indeed, a fusion zone, a heat affected zone and regions of the basic

ISSN 1737-9296

materials are distinguished. The difference in thermal and physical properties in the solid and the liquid states of base metals such as specific heat capacity, melting temperature, densities and thermal diffusivity affects the weld bead shape and the depth of penetration.

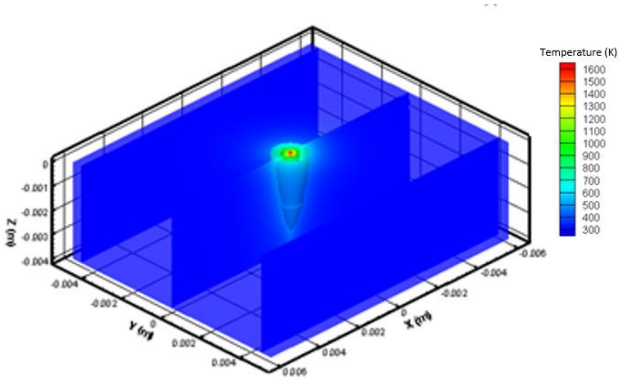

Fig. 1 Isotherms in the workpiece

Figure 2 gives general idea at the distribution of velocity field. It shows the hydrodynamic movements in the melting zone during dissimilar laer welding. Convective movements can be seen. They are important at the free surface than at the interface between the two welded materials. A maximum fluid velocity was obtained at the surface of the weld joint. This is determined by the dominant Marangoni force at the free surface of the weld pool. The Marangoni force depends significantly on the surface tension gradient which itself depends on the temperature gradient created in the melted zone.

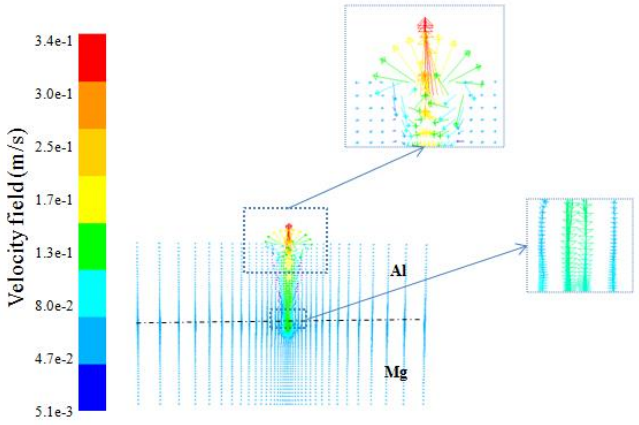

Fig. 2 Contour of velocity field vectors

The distribution of elements in the molten pool contributes to the development of the weld bead. Figures 3 and 4 present the evolution of the mass fraction of Aluminum and Magnesium, respectively during laser welding. A heterogenous mixing zone is formed. Figure 3 indicates that the molten Al alloy descends into the bottom of the weld bead to reach a mass percent of 30% through the hydrodynamic movements generated in the melted pool. The distribution of mass fration of Magnesium shows the displacement of the molten Magnesium alloy to the upper surface via the convective flux (Figure 4). Furthermore, the diffusion phenomenon of Al and Mg alloys profoundly affects the transport of alloying elements in the weld bead.

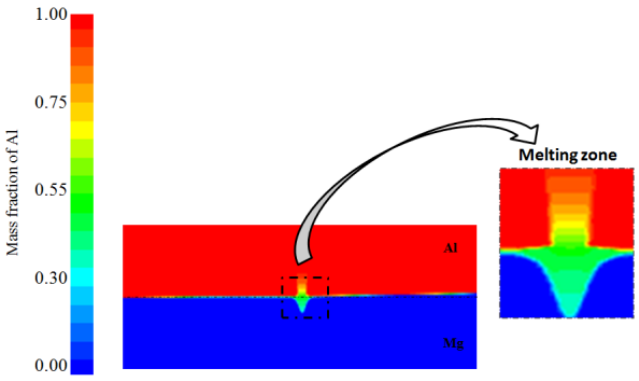

Fig. 3 Cross section of the mass fraction of Aluminum

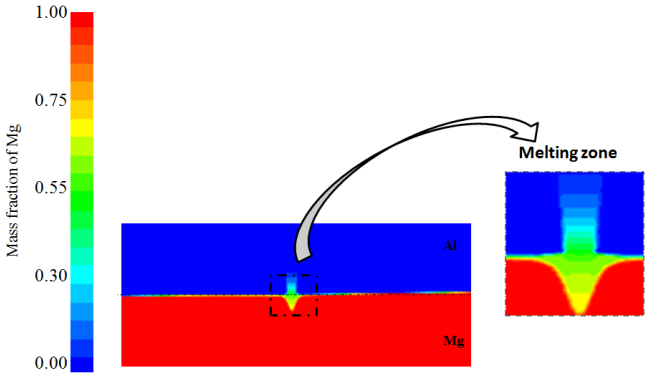

Fig. 4 Cross section of the mass fraction of Magnesium

Figure 6 shows the comparison of chemical distribution of Aluminum and Magnesium obtained experimentally (figure 5) and numerically in the molten zone along a longitudinal line. From Figure 6, the results reveal that the mass percentage of Al varies along the weld bead. The change in the mass fraction of molten Aluminum shows a decrease from the base metal (100 wt%) to the melting zone. On the other hand, the Magnesium content increases in the melting zone. This is due to the hydrodynamic movements created in the molten pool. Hence, the results

ISSN 1737-9296

of the numerical simulation are in agreement with the experimental results.

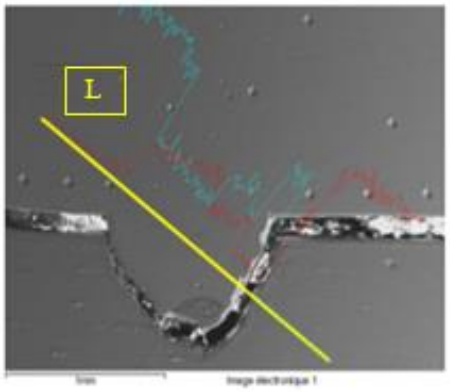

Fig. 5 Experimental profile line of the chemical element distribution in the weld bead

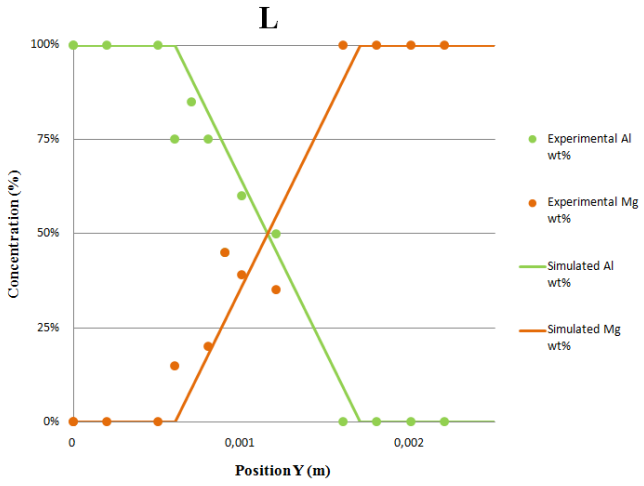

Fig. 6 Experimental and simulated profile lines of Mg and Al distributions

VII. Numerical Validation

Figure 7 shows the comparison of the weld geometry obtained from simulation and experimentation. A good correspondence between the simulated weld bead shape and the experimental results has been seen showing the validity of the predicted model presented in this work.

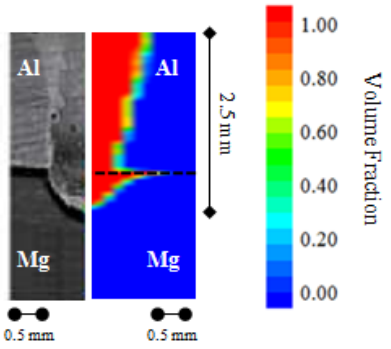

Fig. 7 Comparison of calculated and experimental weld bead shape

VIII. Conclusion

This paper represents a numerical investigation of joining Aluminum and Magnesium alloys by laser. A computational fluid mechanics model analyses the thermal cycle, fluid flow characteristics and keyhole behavior in the molten pool. The results obtained in this work show that thermocapillary forces are generated in the melt pool and contributes to mix molten materials. The convective flows has a significant effect on energy spread. Thermal diffusion leads to transport elements into the weld bead. The calculated results are in good agreement with the experimental results and this validates the 3D multiphysics model developed in this work.

References

[1] R. S. Rana, R. Purohit, and S Das, "Reviews on the Influences of Alloying elements on the Microstructure and Mechanical Properties of Aluminium Alloys and Aluminium Alloy Composites", *International Journal of Scientific and Research Publications*, vol. 2, 2012.

[2] S. Toros, F. Ozturk and I. Kacar, "Review of warm forming of aluminum-magnesium alloys", *J. Mater. Process. Tech.*, vol. 207, pp. 1-12, 2008.

[3] F. Hayat, "The effects of the welding current on heat input, nugget geometry, and the mechanical and fractural properties of resistance spot welding on Mg/Al dissimilar materials", *Mater. Design*, vol. 32, pp. 2476 – 2484, 2011.

[4] G. Casalino, "Statistical analysis of MIG-laser CO_2 hybrid welding of Al-Mg alloy", *J. Mater. Process. Tech.* vol. 191, pp. 106-110, 2007.

[5] C. Liu, D. L. Chen, S. Bhole, X. Cao and Jahazi, *M*, "Polishing-assisted galvanic corrosion in the dissimilar friction stir welded joint of AZ31 magnesium alloy to 2024 aluminium alloy", *Mater. Charact.*, vol. 60, pp. 370-376, 2009.

[6] L. Carrino, A. Squillace, V. Paradiso, S. Ciliberto and M. Montuori, "Superplastic forming of friction stir processed magnesium alloys for aeronautical

ISSN 1737-9296

applications: A modeling approach", *Materials Science Forum*, vol. 735, pp. 180-191, 2013.

[7] L. M. Liu, J. H. Tan, L. M. Zhao and X.J. Liu, "The relationship between microstructure and properties of Mg/Al brazed joints using Zn filler metal", *Mater. Charact*. Vol. 59, pp. 479-483, 2008.

[8] C.T. Chi, C.G. Chao, T. F. Liu, C.H. Lee, "Aluminium element effect for electron beam welding of similar and dissimilar Magnesium–Aluminium–Zinc alloys", *Scr. Mater*., vol. 56, pp. 733–736, 2007.

[9] M Ishak and M. R. Islam, "Weldability of A7075-T651 and AZ31B dissimilar alloys by MIG welding method based on welding appearances", *Journal of Physics*, 2014.

[10] H. T. Zhang and J. Q. Song, "Microstructural evolution of aluminum/magnesium lap joints welded using MIG process with zinc foil as an interlayer", *Mater. Lett.* Vol. 65, pp. 3292-3294, 2011.

[11] F. Hayat, "The effects of the welding current on heat input, nugget geometry, and the mechanical and fractural properties of resistance spot welding on Mg/Al dissimilar materials", *Mater. Des.*, vol. 32, pp. 2476–2484, 2011.

[12] J. Zhang, G. Luo, Y. Wang, Q. Shen and L. Zhang, "An investigation on diffusion bonding of aluminum and magnesium using a Ni interlayer", *Materials Letters*, vol. 83, pp. 189–191, 2012 .

[13] L. Carrino, V. Paradiso, S. Franchitti, A. Squillace and S. Russo, "Superplastic forming/diffusion bonding of a titanium alloy for the realization of an aircraft structural component in multi-sheets configuration", *Key Engineering Materials*, pp. 717-722, 2012.

[14] S. Chen, L. Li, Y. Chen and J. Huanga, "Joining mechanism of Ti/Al dissimilar alloys during laser welding-brazing process", *Journal of Alloys and Compounds*, pp. 891–898, 2011.

[15] G. Casalino, M. Mortello and P. Peyre. "FEM analysis of fiber laser welding of Titanium and Aluminum", *Procedia CIRP*, pp. 992 – 997, 2016.

[16] K. S. Kumar, "Numerical Modeling and Simulation of a Butt Joint Welding Of AISI 316L Stainless Steels Using a Pulsed Laser Beam", *Materials Today: Proceedings*, pp. 2256 – 2266, 2015.

[17] M. F. X. Muthu and V. Jayabalan, "Effect of pin profile and process parameters on microstructure and mechanical properties of friction stir welded Al−Cu joints", *Trans. Nonferrous Met. Soc. China,vol.* 26, pp. 984−993, 2016.

[18] G. Qianqian, L. Jiangqi, Y. Ping, J. Shunchao, H. Wenhao and Z. Jianxi, "Effect of steel to aluminium laser welding parameters on mechanical properties of weld beads", *Optics and Laser Technology*, vol. 111, pp. 387–394, 2019.

[19] S. Bannour, K. Abderrazak, S. Mattei, J. E. Masse, M. Autric, H. Mhiri, "The influence of position in overlap joints of Mg and Al alloys on microstructure and hardness of laser welds", *Journal of laser applications*, vol. 5, 2013.

ISSN 1737-9296